The non-adiabatic hyperspherical approach to the two-dimensional D^- ion in the presence of a magnetic field

2002 J. Phys.: Condens. Matter 14 6841

(http://iopscience.iop.org/0953-8984/14/27/308)

INSTITUTE OF PHYSICS PUBLISHING JOURNAL OF PHYSICS: CONDENSED MATTER

J. Phys.: Condens. Matter **14** (2002) 6841–6853 PII: S0953-8984(02)34883-5

The non-adiabatic hyperspherical approach to the two-dimensional D^- ion in the presence of a magnetic field

A S Santos[1], J J De Groote[2] and L Ioriatti[1]

[1] Instituto de Física de São Carlos, Universidade de São Paulo, Caixa Postal 369, 13560-970 São Carlos, SP, Brazil
[2] Instituto de Química de Araraquara, Universidade Estadual Paulista, Caixa Postal 355, 14800-900 Araraquara, SP, Brazil

E-mail: assantos@if.sc.usp.br

Received 14 March 2002, in final form 1 May 2002
Published 28 June 2002
Online at stacks.iop.org/JPhysCM/14/6841

Abstract

We have used the adiabatic hyperspherical approach to determine the energies and wavefunctions of the ground state and first excited states of a two-dimensional D^- ion in the presence of a magnetic field. Using a modified hyperspherical angular variable, potential energy curves are analytically obtained, allowing an accurate determination of the energy levels of this system. Upper and lower bounds for the ground-state energy have been determined by a non-adiabatic procedure, as the purpose is to improve the accuracy of method. The results are shown to be comparable to the best variational calculations reported in the literature.

1. Introduction

A quasi-two-dimensional centre (D^-) is formed when an extra electron becomes bound to a neutral shallow donor in selectively doped GaAs–GaAlAs multiple-quantum-well structures. For a direct-gap homogeneous semiconductor having a large dielectric constant and small effective mass such as GaAs, the D^- centre may be thought of as an atomic system constituted by two electrons under the Coulomb potential of a single positive ion screened by the dielectric constant of the medium. Since its experimental identification [1–4] in magneto-optical spectra by Huant *et al* [1], a considerable amount of theoretical work has been carried out with the aim of achieving an understanding of this problem [6–19]. Using the Monte Carlo method, for instance, Pang and Louie [6] calculated the electric dipole transition energies of a D^- ion in a quantum well as a function of a magnetic field. Previously, Phelps and Bajaj [5] calculated the ground-state energy of D^- in two dimensions using a variational approach.

Recently, the hyperspherical method was applied to a strictly two-dimensional D^- ion by Ruan *et al* [19] in the calculation of the ground state and first excited states of a strictly two-dimensional (2D) D^- system. Like the traditional adiabatic Born–Oppenheimer approach, the hyperspherical adiabatic method is based on the determination of radial-like potential curves from which one can determine not only the ground state, but also excited states. This method has been successfully applied to a variety of few-body atomic and molecular systems [20–31].

In this paper, we have applied the hyperspherical approach to calculate precise bound-state energies for the 2D D^- system in the presence of a static magnetic field perpendicular to the plane in which the electrons are confined. In contrast to Ruan *et al* [19], we have solved the system of equations of the hyperspherical (HS) adiabatic method by using a different HS angular variable [22]. The introduction of this variable allows an analytical solution of the HS angular coupled equations through an expansion of the HS angular wavefunctions in a fast-converging power series, applying the Fröbenius method. As a result we have obtained precise potential curves, which is a pre-condition for an accurate determination of energies and radial wavefunctions. To further improve the precision of our results, we have introduced the non-adiabatic couplings in the radial equation solution. The $M = 0$ and 1 binding energies and energy transition obtained in this way have precisions that are comparable to the those of best variational results found in the literature (see e.g. [8]).

The introduction of the hyperspherical adiabatic approach in the study of two-dimensional systems is motivated by the good results obtained for strongly correlated three-dimensional systems [20–31]. This approach allows a very precise *ab initio* procedure in which upper and lower bounds for the exact energy are obtained [32, 33]. The HS coordinates correlate the electronic radial variable in such a way that all the new variables are compact, except for a unique radial variable, called the hyperradius R. This variable is related to the sum of the squares of all radial components, which in turn is related to the electronic inertia moment of the system. This characteristic can be explored to set up an adiabatic procedure in which the angular part of the Schrödinger equation is solved for fixed values of R, resulting in potential curves and non-adiabatic couplings for the radial equation. The procedure is similar to the Born–Oppenheimer approach for diatomic molecules. It is the use of the potential curves picture which turns the HS method into an intuitive procedure and, most importantly, the precision can be controlled just by varying the number of coupled radial channels. It turns out that the results obtained with only the simplest approximation, in which all the radial couplings are disregarded, are sufficient to produce the ground-state energy with errors of only 1% [28]. The precision is increased by a factor of ten by just introducing the first diagonal non-adiabatic coupling [22]. The results obtained for the two-dimensional D^- system show that the HS method is also precise, with a precision of convergence similar to that observed for other three-dimensional equivalent systems. To improve the precision, it is only necessary to introduce upper potential curves for the radial equation and the appropriate couplings. Following this procedure, the energy obtained will approach the exact one until the desirable precision is achieved. It is important to point out that the procedure does not have adjustable parameters.

In the following sections we will present the mathematical details of the method and the results obtained for the 2D D^- system.

2. The bi-dimensional hyperspherical adiabatic approach

With the notion that the electrons in semiconductors can be described as having a conduction band effective mass m, and their motion confined to a plane, under a magnetic field perpendicular to the plane, energy levels and wavefunctions are given by the following

Schrödinger equation:

$$\left[\nabla_1^2+\nabla_2^2+\frac{2Z}{r_1}+\frac{2Z}{r_2}-\frac{2}{|\vec{r}_1-\vec{r}_2|}-\gamma(L_{z1}+L_{z2})-\frac{\gamma^2}{4}(r_1^2+r_2^2)+2E\right]\Psi(\vec{r}_1,\vec{r}_2)=0 \tag{1}$$

where are have set $\hbar=e=m=1$ and $L_{zi}=-\mathrm{i}\,\partial/\partial\varphi_i$, $i=1,2$, are the individual electron azimuthal angular momentum operators, in units of $\hbar$. The magnetic field appears in the dimensionless parameter

$$\gamma=\frac{\hbar\omega_c}{2\,\mathrm{Ryd}}, \tag{2}$$

given by the ratio of magnetic field energy to two rydbergs and $\omega_c=\frac{eB}{mc}$ is the electron cyclotron frequency. The D^- centre with charge Ze is considered to be at the centre of mass.

In this work only D^- spin-singlet states are considered—that is, antisymmetric spin wavefunctions corresponding to the total spin quantum number $S=0$.

The radial polar coordinates can be transformed into the hyperspherical [34] ones by means of the following relations:

$$\begin{aligned} R\sin\alpha&=r_1\\ R\cos\alpha&=r_2. \end{aligned} \tag{3}$$

The hyperspherical wavefunction is written as

$$\psi(R,\Omega)=(R^3\sin\alpha\cos\alpha)^{1/2}\Psi(R,\Omega), \tag{4}$$

where $\Omega=\{\alpha,\varphi_1,\varphi_2\}$ represents the new set of compact variables.

Using these variables, the Schrödinger equation will assume the form

$$\left[\frac{\partial^2}{\partial R^2}+\frac{1}{4R^2}+\frac{1}{R^2}\hat{U}(R,\Omega)-\frac{\gamma^2}{4}R^2+2\varepsilon\right]\psi(R,\Omega)=0. \tag{5}$$

Since the total angular momentum operators appearing in equation (1) commute with the total Hamiltonian, they can be diagonalized separately in terms of the total azimuthal angular momentum. For this reason, the total energy E can be redefined as $\varepsilon=E-\gamma M/2$, where M is the total azimuthal quantum number. The angular operator $\hat{U}(R,\Omega)$ contains a simple linear dependence on R, which multiplies all the interaction terms. Its explicit form is

$$\hat{U}(R,\Omega)=\frac{\partial^2}{\partial\alpha^2}-\frac{L_{z1}^2-1/4}{\sin^2\alpha}-\frac{L_{z2}^2-1/4}{\cos^2\alpha}+\frac{2ZR}{\sin\alpha}+\frac{2ZR}{\cos\alpha}-\frac{2R}{\sqrt{1-\sin 2\alpha\cos\varphi_{12}}}$$

where $\cos\varphi_{12}=\hat{r}_1\hat{r}_2$.

The angular operator is Hermitian and therefore, for each value of R, it has a complete set of eigenfunctions called channel functions:

$$\hat{U}(R,\Omega)\Phi_\mu(R;\Omega)=U_\mu(R)\Phi_\mu(R;\Omega). \tag{6}$$

As R varies, the eigenvalues $U_\mu(R)$ will form continuous potential curves. The adiabatic procedure consists in the expansion of the normalized total wavefunction in the basis formed by the angular channel functions [34], written as

$$\psi(R,\Omega)=\sum_\mu F_\mu(R)\Phi_\mu(R;\Omega). \tag{7}$$

The substitution of this expansion into equation (5) results in a set of coupled radial equations:

$$\left(\frac{\mathrm{d}^2}{\mathrm{d}R^2}+\frac{U_\mu(R)+1/4}{R^2}-\frac{\gamma^2R^2}{4}+2\varepsilon\right)F_\mu(R)+\sum_\upsilon\left(2P_{\mu\upsilon}(R)\frac{\mathrm{d}}{\mathrm{d}R}+Q_{\mu\upsilon}(R)\right)F_\upsilon(R)=0 \tag{8}$$

where

$$P_{\mu\upsilon}(R) = \left\langle \Phi_\mu(R;\Omega) \middle| \frac{\partial}{\partial R}\Phi_\upsilon(R;\Omega) \right\rangle, \tag{9}$$

$$Q_{\mu\upsilon}(R) = \left\langle \Phi_\mu(R;\Omega) \middle| \frac{\partial^2}{\partial R^2}\Phi_\upsilon(R;\Omega) \right\rangle. \tag{10}$$

are the non-adiabatic couplings. The brackets in these equations represent integration over the angular variables.

The solution of the HS Schrödinger equation is now separated into two parts. Initially the potential curves and the non-adiabatic couplings of the angular equations are obtained and afterwards, using these results, the radial equation is solved. Since the radial equation is an infinite system of coupled differential equations, it has to be truncated. This is achieved by imposing a maximum number μ_{max} on the expansion of the total wavefunction in equation (7). The exact energy will be approached in a systematic way by gradually increasing μ_{max}. The simplest radial approximation corresponds to the complete disregard of all couplings, and leads to a simple one-dimensional radial equation. This approximation, referred to as the extreme uncoupled adiabatic approach (EUAA), has the property of furnishing an approximate energy (E_{EUAA}) representing a lower bound on the exact one (ε) [32,33]. The inclusion of the diagonal coupling will raise the energy to an upper bound (E_{UAA}). This approximation is referred to as the uncoupled adiabatic approach (UAA). The inclusion of non-diagonal couplings, the coupled adiabatic approach (CAA), will also give upper bounds on the exact energy in such a way that, as the number of coupled radial components is increased, the energy E_{CAA} will become closer to the exact one. The advantage of this procedure is that it allows control of the energy precision up to a desired point, with the benefit that the simplest adiabatic approximation is enough to give binding energies with good precision, even for excitons bound to donor impurities, which have small binding energies [23, 27, 31]. In order to achieve accurate results using the HS adiabatic method, good quality of the HS angular solution is essential. This is discussed in the next section.

3. Hyperspherical angular equation

Initially the channel functions are expanded in the coupled angular wavefunctions of particles 1 and 2:

$$\Phi_\mu(R;\Omega) = \frac{1}{2\pi}\sum_{m_1 m_2} G^\mu_{M m_1 m_2}(R;\alpha)\exp(\mathrm{i}m_1\varphi_1)\exp(\mathrm{i}m_2\varphi_2), \tag{11}$$

which diagonalizes the individual angular operators L_z^2. The quantum numbers m_1 and m_2 are the electronic magnetic momenta and $M = m_1 + m_2$ is the total magnetic momentum. With the use of the antisymmetrization Pauli principle it is possible to impose a contour condition [22,34] for the HS angular channels at $\alpha = \pi/4$, which corresponds to the point where the electrons are at the same distance from the nucleus. For this value of α the components $G^\mu_{M m_1 m_2}(R;\alpha)$ of the angular channels must be obey the following conditions:

$$\begin{aligned} &G^\mu_{M m_1 m_2}(R;\pi/4) = (-1)^{S_z} G^\mu_{M m_2 m_1}(R;\pi/4), \\ &\left(\frac{\partial}{\partial\alpha} G^\mu_{M m_1 m_2}(R;\alpha)\right)_{\pi/4} = -(-1)^{S_z}\left(\frac{\partial}{\partial\alpha} G^\mu_{M m_2 m_1}(R;\alpha)\right)_{\pi/4}, \end{aligned} \tag{12}$$

where S_z is the total electronic spin. Substituting the expansion of equation (11) into the angular equation results in the following differential equation:

$$\left(\frac{\partial^2}{\partial\alpha^2} - \frac{(m_1^2-1/4)}{\sin^2\alpha} - \frac{(m_2^2-1/4)}{\cos^2\alpha} + \frac{2ZR}{\sin\alpha} + \frac{2ZR}{\cos\alpha} - U_\mu(R)\right) G^\mu_{Mm_1m_2}(R;\alpha) - \frac{2R}{\cos\alpha}\sum_{j,m_1'm_2'} \tan^j\alpha C^\mu(M,m_1,m_2,m_1',m_2',j) G^\mu_{Mm_1'm_2'}(R;\alpha) = 0. \tag{13}$$

This set of differential equations is infinitely coupled, and is truncated to a finite number of components of the function $G^\mu_{Mm_1m_2}(R;\alpha)$ by selecting a maximum value m_{max} for m_1 and m_2 in the expansion of $\Phi_\mu(R;\Omega)$.

The coupling constant C^μ is given by the expression

$$C^\mu(M,m_1,m_1',j) = 2^{-j}\sum_{n=n_0}^{j}(-)^k 2^{-n}\frac{(n+j)!}{\left(\frac{n-\Delta m_1}{2}\right)!\left(\frac{n+\Delta m_1}{2}\right)!\left(\frac{j-n}{2}\right)!\left(\frac{j+n}{2}\right)!}$$

where, $n_0 = j - 2\left[\frac{j}{2}\right]$, $k = \frac{j-n}{2}$ and $\Delta m_1 = m_1 - m_1'$.

The poles at $\alpha = 0$ and $\pi/2$ are considered by changing the wavefunction into the form

$$G^\mu_{Mm_1m_2}(R;\alpha) = (\sin\alpha)^{|m_1|+1/2}(\cos\alpha)^{|m_2|+1/2}\mathrm{e}^{p\alpha}H^\mu_{Mm_1m_2}(R;\alpha) \tag{14}$$

where

$$p = -\frac{ZR}{n_\mu} \tag{15}$$

and $n_\mu = N + 1/2$, where $N = 1, 2, 3, \ldots$ is the asymptotic hydrogenic principal quantum number in two dimensions. The exponential term was added to improve the convergence at large R of the angular channels, in which one electron is scattered with zero energy, and the second is bound to the D^- centre forming a hydrogen-like atom. The resulting equation is

$$\left\{\frac{\partial^2}{\partial\alpha^2} + 2[(|m_1|+1/2)\cot\alpha - (|m_2|+1/2)\tan\alpha + P]\frac{\partial}{\partial\alpha} + \frac{2ZR}{\sin\alpha} + \frac{2ZR}{\cos\alpha} + p^2 + 2p[(|m_1|+1/2)\cot\alpha - (|m_2|+1/2)\tan\alpha] - (|m_1|+|m_2|+1)^2 - U_\mu(R)\right\} \times H^\mu_{Mm_1m_2}(R;\alpha) - \frac{2R}{\cos\alpha}\sum_{jm_1'm_2'}\tan^j\alpha(\sin\alpha)^{|m_1'|-|m_1|} \times (\cos\alpha)^{|m_2'|-|m_2|}C^\mu(M,m_1,m_1',j)H^\mu_{Mm_1'm_2'}(R;\alpha) = 0. \tag{16}$$

In this equation the m_2-index was removed from the summation index since it can be related to M and m_1 through the relation $m_2 = M - m_1$.

3.1. Polynomial representation of the angular equation

The change from the trigonometric coefficients of the HS angular equation to rational ones is achieved replacing the α-coordinate by [22]

$$x = \tan(\alpha/2). \tag{17}$$

The resulting new equation coefficients are rational functions, which allows solution of the wavefunction by a fast-converging recursion series, through the Fröbenius method.

With this variable, the solution at $R = 0$ is no longer polynomial. This can be corrected with a last modification of the angular wavefunction:

$$T^\mu_{Mm_1m_2}(R,\alpha) = (1+x^2)^{-S}H^\mu_{Mm_1m_2}(R,\alpha) \tag{18}$$

where

$$S = |m_1| + |m_2| + 1 - \mu_0 \tag{19}$$

is chosen for the angular solution being calculated, which defines μ_0 as the solution in $R = 0$ of the angular channel. This modification improves the numerical results for small values of R. The resulting equation can be organized into a compact form:

$$\left[A(x)\frac{\partial^2}{\partial x^2} + B(x, m_1, m_2)\frac{\partial}{\partial x} + C(x, m_1, m_2)\right]T^{\mu}_{Mm_1m_2} = \sum_{m_1'm_2'} D(x, m_1, m_2, m_1', m_2')T^{\mu}_{M,m_1'm_2'} \tag{20}$$

where the coefficients are defined below:

$$A(x) = -x^7 - x^5 + x^3 + x, \tag{21}$$

$$B(x, m_1, m_2) = 2|m_1| + 1 + 4xp + (-2|m_1| - 8|m_2| - 4S - 3)x^2 + (-5 - 2|m_1| - 8|m_2|)x^4 - 4x^5p + (-1 + 2|m_1| + 4S)x^6, \tag{22}$$

$$\begin{aligned} C(x, m_1, m_2) = {} & 2(1 + 2|m_1|)p + 4ZR + (4p^2 + 8ZR - 4U_\mu - 4(|m_1| + 1)S \\ & - 4(|m_1| + |m_2| + 1)^2)x + p(-12 - 16|m_2| - 8|m_1| - 8S)x^2 \\ & + 4(U_\mu + 2ZR - p^2 + S(S + 1) + (|m_1| + |m_2| + 1)^2 \\ & + 2Sa(1 + |m_1| + 2|m_2|)x^3 \\ & + (-4ZR + 2p(4S + 2|m_1| + 1))x^4 - 4S(S + |m_1|)x^5, \end{aligned} \tag{23}$$

and

$$\begin{aligned} D(x, m_1, m_2, m_1', m_2') = {} & R(1 + x^2)\sum_j 2^{3+j+|m_1'|-|m_1|}x^{1+j+|m_1'|-|m_1|} \\ & \times (1 - x^2)^{|m_2'|-|m_2|-j}C^{\mu}(M, m_1, m_1', j). \end{aligned} \tag{24}$$

These coefficients may be written in a compact form as

$$A(x) = \sum_{i=0}^{N_a} a(i)x^i \tag{25}$$

$$B(x, m_1, m_2) = \sum_{i=0}^{N_b} b(i, m_1, m_2)x^i \tag{26}$$

$$C(x, m_1, m_2) = \sum_{i=0}^{N_c} c(i, m_1, m_2)x^i. \tag{27}$$

The coupling term $D(x, m_1, m_2, m_1', m_2')$ can also be written in powers of the variable x by expanding the $(1 - x^2)$ term of equation (24) as

$$(1 - x^2)^{|m_2'|-|m_2|-j} = \sum_{k=0}^{k_{max}} q(k, m_2, m_2', j)x^{2k}, \tag{28}$$

where:

$$\begin{aligned} &\text{if } (|m_2'| - |m_2| - j) \geqslant 0 \qquad \begin{cases} k_{max} = |m_2'| - |m_2| - j, \\ q(k, m_2, m_2', j) = (-1)^k \begin{pmatrix} |m_2'| - |m_2| - j \\ k \end{pmatrix}; \end{cases} \\ &\text{if } (|m_2'| - |m_2| - j) < 0 \qquad \begin{cases} k_{max} = \text{arbitrary}, \\ q(k, m_2, m_2', j) = \begin{pmatrix} -|m_2'| + |m_2| + j + k - 1 \\ k \end{pmatrix}. \end{cases} \end{aligned} \tag{29}$$

We have then

$$D(x, m_1', m_1, M) = R(1+x^2)\sum_{j=0}^{j_{max}} 2^{3+j+|m_1'|-|m_1|}\sigma^{j-1}C^{\mu}(M, m_1, m_1', j) \times \sum_{k=0}^{k_{max}} q(k, m_1, m_1', M, j)x^{2k+1+j+|m_1'|-|m_1|}. \tag{30}$$

The resulting expression for $D(x, m_1', m_1, M)$ is

$$D(x, m_1', m_1, M) = \sum_{i=0}^{Nd} d(i, m_1', m_1, M)x^i. \tag{31}$$

Now, expanding the total wavefunction as a power series in the variable x:

$$T^{\mu}_{Mm_1m_2} = \sum_n t(\mu, M, m_1, m_2, n)x^n \qquad \text{or just} \qquad \sum_n t(m_1, m_2, n)x^n \tag{32}$$

we get the recursion relationship

$$\begin{aligned}-[n(n+1)a(1) + nb(0, m_1, m_2)]t(m_1, m_2, n) &= \sum_{i=2}^{N_a} n(n+1)a(i)t(m_1, m_2, n+1-i) \\ &+ \sum_{i=1}^{N_b} nb(i, m_1, m_2)t(m_1, m_2, n-i) + \sum_{i=0}^{N_c} c(i, m_1, m_2)t(m_1, m_2, n-1-i) \\ &+ \sum_{m_1'm_2'}\sum_{i=0}^{Nd} C^{\mu}(M, j, m_1, m_1')\mathrm{d}(i, m_1', m_1, M)t(m_1', m_2', n-1-i) \\ &+ \sum_{m_1'm_2'}\sum_{i=0}^{Nd} C^{\mu}(M, j, m_1, m_1')\mathrm{d}(i, m_1', m_1, M)t(m_1', m_2', n-3-i). \end{aligned} \tag{33}$$

4. Numerical analysis

The hyperspherical adiabatic procedure developed in the last section is an exact one. However, as discussed above, some approximations will have to be made. The expansion of the HS wavefunction in angular channel components in equation (7) will be truncated, limiting to μ_{max} the number of coupled radial components in the radial equation. The number of coupled angular components of the angular equation, referred to as N_C, will also be restricted by limiting the sum over m_1 and m_2 in the expansion of the angular channels in polar angular wavefunctions (equation (11)), and it will be necessary to impose a limit j_{max} on the number of terms used to expand the electron–electron (e–e) interaction in equation (13).

The initial numerical algorithm test performed on the HS angular equation was accomplished by the numerical checking of the first derivative of the potential curves at small values of R. This result confirmed our calculations when compared with analytical results obtained by first-order perturbation theory at $R = 0$ using the exact angular channels of this limit, given as

$$\frac{\partial U}{\partial R} = \int\left(\frac{4}{\sin\alpha} + \frac{4}{\cos\alpha} - \frac{2}{\cos\alpha}\sum_{j=0}^{j_{max}}\tan^j\alpha P_j(\cos\varphi_{12})\right)(G^{\mu}_{Mm_1m_2}(0,\alpha))^2\,\mathrm{d}\Omega \tag{34}$$

where the $R = 0$ angular channel wavefunction is

$$G^{\mu}_{Mm_1m_2}(0;\alpha) = (\sin\alpha)^{|m_1|+1/2}(\cos\alpha)^{|m_2|+1/2}P_{\nu}^{(|m_1|,|m_2|)}(\cos 2\alpha), \tag{35}$$

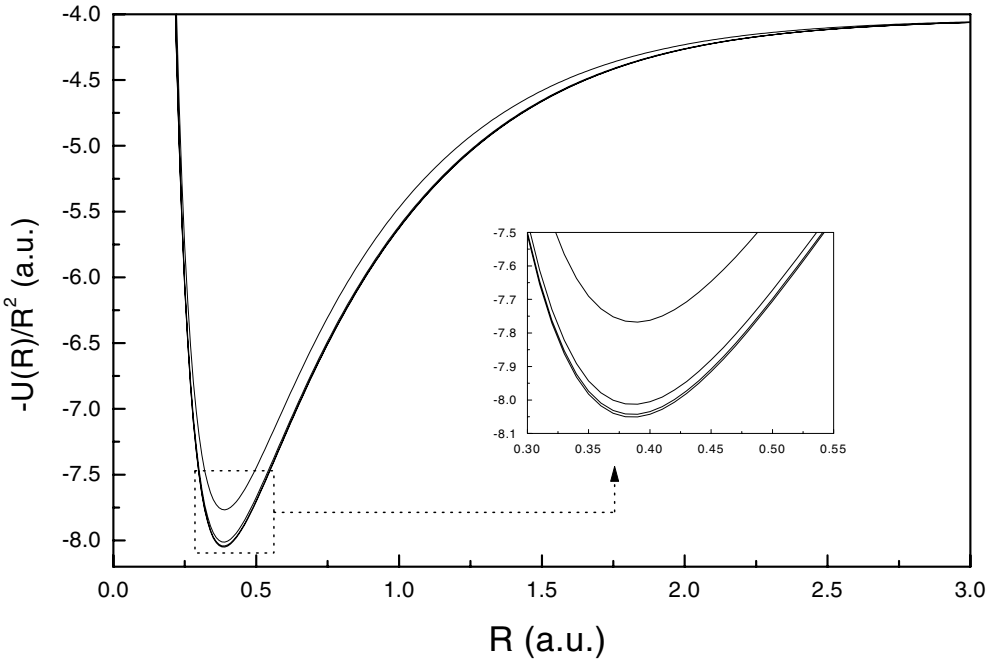

Figure 1. D^- potential curve convergence for $N_C = 1, 3, 7, 9$. The minimum is lowered as N_C increases.

with the eigenvalues

$$U_\mu(0) = -(2\nu + |m_1| + |m_2| + 1)^2. \tag{36}$$

The terms $P_\nu^{(|m_1|,|m_2|)}$ are Jacobi polynomials ($\nu = 0, 1, 2, \ldots$) [34].

The results for large values of R were also correct, with the potential curves behaving as predicted by the theoretical calculations for the asymptotic limit; that is,

$$\lim_{R\to\infty} U_\mu(R) = \frac{(ZR)^2}{(n + |m_1| + 1/2)^2}, \qquad n = 0, 1, \ldots. \tag{37}$$

For the energy calculations throughout this work, the sum on the e–e coupling will be made adopting the value $j_{max} = 35$, in order to guarantee that the most important parameter is the number of coupled angular channels, since it is related to a slower energy convergence from the numerical effort point of view.

We have also checked the convergence of the first potential curve as a function of the number of angular coupled channels N_C. The results are summarized in figure 1, where we can see how the potential curve minimum is affected. In this figure, the lowest curves are the ones with the larger values of N_C. This figure also shows that it is in the region of the minimum that the discrepancy between the curves is largest. The results are stable, showing a fast convergence. The value $N_C = 9$, based on these results, will be adopted throughout this work.

4.1. Non-adiabatic energies

In this section we analyse the effect on the ground-state energy of the inclusion of non-adiabatic couplings. The adiabatic approximation procedure produces potential curves related to each set

of quantum numbers of the angular equation, $\mu = (m_1, m_2, \nu)$, as given in equation (36). When the non-adiabatic couplings of the radial equation are disregarded, each of these potential curves has associated eigenstates, which are independent of the eigen-solutions obtained from other potential curves. The importance of the hyperspherical coordinate choice for the description of atomic systems resides in the fact that the hyperradial variable is a good adiabatic parameter, as reflected in the small contribution of the non-adiabatic couplings to the radial equation. As a result, the introduction of the couplings produces small corrections to the energy, thus yielding very precise results with only a few coupled radial channels.

The diagonal term, $Q_{11}(R)$ (equation 10), is the most important coupling, since it is responsible for the major contribution to the energy convergence.

An important aspect related to Q_{11} is the relation of the boundaries for the exact energy values generated by the energies obtained with (ε_{UAA}) and without (ε_{EUAA}) its inclusion, as given below:

$$\varepsilon_{EUAA} \leqslant \varepsilon \leqslant \varepsilon_{UAA}. \tag{38}$$

Since the effect of Q_{11} when added to the potential curve is small, the energy is confined to a region delimited by an error that is usually smaller than 1% for two-electron systems [26]. However, the error is in fact smaller, because the inclusion of non-adiabatic couplings makes the energy closer to the exact value. This means that the Q_{11}-term produces an upper-bound limit, which is closer to the exact result than the lower bound. An improvement is obtained when non-diagonal couplings are introduced, and errors drop rapidly following the relationship

$$\varepsilon_{EUAA} \leqslant \varepsilon \leqslant \varepsilon_{CAA} \leqslant \varepsilon_{UAA}. \tag{39}$$

In order to check the results for the ground state for the two-dimensional D^- ion, we have used for comparison the precise variational data (E_{var}) from Phelps and Bajaj [5]:

$$E_{UAA} = -4.474\,65 \text{ Ryd} \qquad (\mu_{max} = 1)$$
$$E_{CAA} = -4.481\,50 \text{ Ryd} \qquad (\mu_{max} = 2)$$
$$E_{CAA} = -4.481\,67 \text{ Ryd} \qquad (\mu_{max} = 3)$$
$$E_{EUAA} = -4.575\,36 \text{ Ryd} \qquad (\mu_{max} = 1)$$
$$E_{var} = -4.480\,1 \text{ Ryd}.$$

The EUAA and UAA energy approximations have correctly bounded the variational energy, and the UAA error is only 0.1%, which is an excellent result considering that only a simple uncoupled radial equation was solved. On coupling three radial channels this error drops to 0.04%. This energy is lower than the variational energy, which is consistent with the precision of the variational functions used by Phelps and Bajaj [5]. Such functions were tested for the H^- ion, leading to a ground-state energy of 1.055 34 Ryd, while the very accurate value from Pekeris [35] is 1.0555 Ryd. The result obtained in this work for three HS radial coupled channels is 1.055 42 Ryd, which is also more precise than the result of [5]. With 13 coupled radial channels, the HS non-adiabatic energy error drops to only 4 ppm. Similar results have been obtained for other helium-like ions [26, 30].

The use of the HS angular channels power series expansion in terms of the variable $x = \tan\alpha/2$ is an important aspect of the method, since it allows a precise determination of the non-adiabatic couplings. The diagonalization of the HS angular operator may also be performed in the determination of qualitative results, as in [19], where energies from approaches equivalent to our EUAA and UAA have been calculated.

For the $M = 1$ state the lowest potential curves behave as anti-bonding molecular orbital potential curves. As a result, there is no bound state. This may be understood in terms

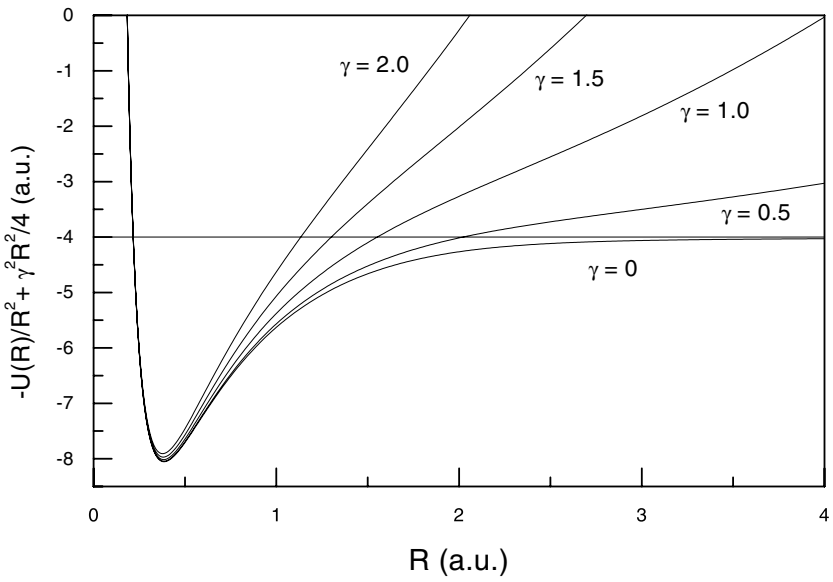

Figure 2. The effect of the hyperradial parabolic term of the Hamiltonian due to the magnetic field is added to the lowest $M = 0$ potential curve.

Table 1. Ground-state energy convergence within the hyperspherical approximation, compared with the variational result of [8] in rydbergs (Ryd).

γ	E_{EUAA}	E_{UAA}	$E_{CAA}(\mu_{max} = 2)$	$E_{CAA}(\mu_{max} = 3)$	E_{var}
0.0	−4.575 361	−4.474 651	−4.481 501	−4.481 668	−4.478
0.5	−4.440 382	−4.339 634	−4.347 200	−4.347 404	−4.346
1.0	−4.132 499	−4.035 238	−4.042 433	−4.042 684	−4.042
2.0	−3.258 710	−3.170 252	−3.175 104	−3.175 425	−3.172
4.0	−0.999 903	−0.922 835	−0.924 967	−0.925 373	−0.917

of the more effective shielding of the nuclear charge exerted by one of the electrons when compared with the three-dimensional equivalent system, which also has only one bound state. The consequence is the absence of $M = 0 \rightarrow 1$ electric dipole transitions. These transitions, however, can be produced through the introduction of an external magnetic field; this is analysed next.

The potential curves obtained in the previous section are not affected by the hyperradial parabolic term $\gamma^2 R^2/4$ added to the Hamiltonian due to the presence of a magnetic field (equation (5)). The potential energy for the radial equation corresponds then to the sum of their contributions, as indicated in figure 2. The resulting behaviour of the energy for different values of γ is shown in table 1 for the lowest $M = 0$ potential curve within the EUAA, UAA and CAA approximations up to three coupled radial channels. We observe that two coupled radial channels are sufficient to provide energies lower than the variational results of Larsen and McCann [8] for all values of γ in table 1. This result is related to the simplified 11-parameter trial wavefunction used by these authors. For $\gamma = 0$ their result for the ground-state energy is 4.478 Ryd while the 35-term trial function result from Phelps and Bajaj [5] is −4.4801 Ryd.

The effect of a magnetic field on the $M = 1$ potential curve is shown in figure 3. The presence of the parabolic potential allows the existence of $M = 1$ bound states, whose energies

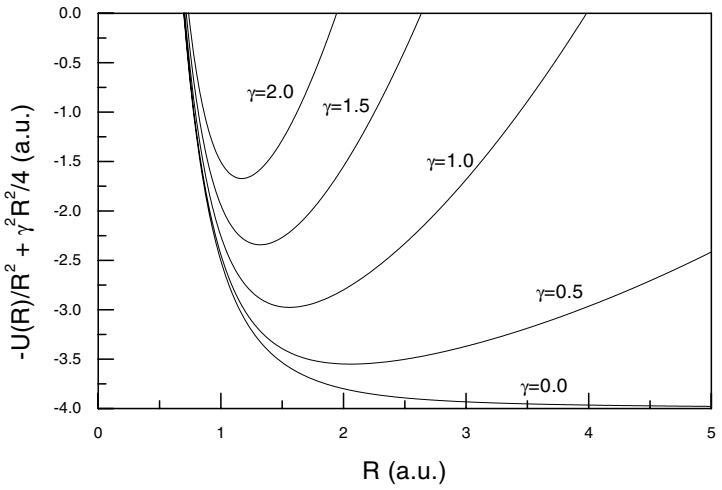

Figure 3. The effect of the hyperradial parabolic term of the Hamiltonian due to the magnetic field on the lowest $M = 1$ potential curve.

Table 2. $M = 1$ lower-state energy convergence within the hyperspherical approximation, compared with the variational result of [8], in Ryd.

γ	E_{EUAA}	E_{UAA}	$E_{CAA}(\mu_{max} = 2)$	$E_{CAA}(\mu_{max} = 3)$	E_{var}
0.5	−3.492 268	−3.420 811	−3.426 676	−3.427 098	−3.430
1.0	−2.875 823	−2.769 353	−2.784 363	−2.784 750	−2.789
2.0	−1.506 703	−1.364 191	−1.395 346	−1.396 529	−1.399
4.0	1.493 931	1.659 955	1.611 59	1.608 605	1.615

are shown in table 2. In this case, the results of [8] are lower, although the energy difference from the HS result with three coupled radial channels is smaller than 0.005 Ryd.

The $M = 0 \rightarrow 1$ energy transition ΔE shown in table 3 as a function of γ is in good agreement with the variational result of Larsen and McCann [8], showing the consistency of the hyperspherical adiabatic procedure developed in this work.

A useful aspect of the HS adiabatic approach is that the potential curves and non-adiabatic couplings are independent of the energy and magnetic field. These HS functions, whose calculation constitutes most of the numerical work, have to be calculated only once. The determination of the radial solutions is very fast from the numerical point of view, and does not compromise the accuracy of the results, as observed on comparison with the variational calculation involving a large number of adjustable parameters. The adiabatic procedure with the direct solution of the coupled HS differential equations is also efficient when compared with the diagonalization process, where a large numerical effort is necessary to obtain qualitative numerical results, as shown in [36].

5. Conclusions

In this work a hyperspherical adiabatic procedure was used to analyse the two-dimensional D^- system. By using the intuitive picture of potential curves, the method was proven to also be very accurate. Our results for the ground state of the D^- centres are in good agreement with the variational results reported in the literature, even in the presence of magnetic fields.

Table 3. Behaviour of the bound energies of D^- as the magnetic field changes. The energies were obtained with three coupled radial channels ($\mu_{max} = 3$).

γ	$E(M = 0)$ (Ryd)	$E(M = 1)$ (Ryd)	ΔE (Ryd)
0.0	−4.481 668	—	—
0.1	−4.475 304	−3.894 588	0.580 716
0.2	−4.457 091	−3.783 417	0.673 674
0.3	−4.428 722	−3.667 986	0.760 736
0.4	−4.391 751	−3.549 027	0.842 724
0.5	−4.347 404	−3.427 098	0.920 306
0.6	−4.296 643	−3.302 623	0.994 020
0.7	−4.240 228	−3.175 926	1.064 302
0.8	−4.178 773	−3.047 257	1.131 516
0.9	−4.112 784	−2.916 812	1.195 972
1.0	−4.042 684	−2.784 750	1.257 934
1.1	−3.968 833	−2.651 201	1.317 632
1.2	−3.891 538	−2.516 276	1.375 262
1.3	−3.811 066	−2.380 069	1.430 997
1.4	−3.727 651	−2.242 661	1.484 990
1.5	−3.641 498	−2.104 125	1.537 373
1.6	−3.552 790	−1.964 524	1.588 266
1.7	−3.461 690	−1.823 914	1.637 776
1.8	−3.368 344	−1.682 348	1.685 996
1.9	−3.272 882	−1.539 872	1.733 010
2.0	−3.175 425	−1.396 529	1.778 896
4.0	−0.925 373	1.608 605	2.533 978

The efficiency of the procedure is due to the good adiabatic variable chosen, which allows small non-adiabatic couplings for the HS radial equation. A single potential curve, in which all couplings are neglected, is enough to give a binding energy with only 2% error. With the inclusion of the diagonal non-adiabatic coupling, this error drops to 0.1%. The inclusion of a magnetic field affects only the HS radial equation through a simple parabolic potential in the hyperradial variable, and leaves the potential curves and non-adiabatic couplings unchanged. This reduces the numerical work, and the error accumulation. With the inclusion of the non-diagonal non-adiabatic couplings, the energy accuracy is improved, approaching the exact value in a systematic way through upper-bound limits. With three coupled radial channels, the energy error drops to only 0.04%. More couplings would give even better results, but for the purposes of this work the accuracy obtained is enough, considering the approximation involving the strictly two-dimensional potentials.

Acknowledgments

The authors would like to thank Fundação de Amparo à Pesquisa do Estado de São Paulo (FAPESP, Brazil) for financial support, under Process No 97/06271-1. ASS would also like to acknowledge the financial support from CNPq and Capes (Brazilian agencies).

References

[1] Huant S, Najda S P and Etienne B 1990 *Phys. Rev. Lett.* **65** 1486
[2] Holmes S, Cheng J-P, McCombe B D and Schaff W 1992 *Phys. Rev. Lett.* **69** 2571
[3] Huant S, Mandray A, Zhu J, Louie S G, Pang T and Etienne B 1993 *Phys. Rev.* B **48** 2370

[4] Kono J, Lee S T, Salib M S, Herold G S, Petrou A and McCombe B D 1996 *Solid-State Electron.* **40** 93
[5] Phelps D E and Bajaj K K 1983 *Phys. Rev.* B **27** 4883
[6] Pang T and Louie S G 1990 *Phys. Rev. Lett.* **65** 1635
[7] Larsen D M and McCann S Y 1992 *Phys. Rev.* B **45** 3485
[8] Larsen D M and McCann S Y 1992 *Phys. Rev.* B **46** 3966
[9] Mueller E R, Larsen D M, Waldman J and Goodhue W D 1992 *Phys. Rev. Lett.* **68** 2204
[10] Xia X and Quinn J J 1992 *Phys. Rev.* B **46** 12 530
[11] MacDonald A H 1992 *Solid State Commun.* **84** 109
[12] Dzyubenko A B 1992 *Phys. Lett.* A **165** 357
[13] Dzyubenko A B and Sivachenko A Yu 1993 *Phys. Rev.* B **48** 14 690
[14] Blinowski J and Szwacka T 1994 *Phys. Rev.* B **49** 10 231
[15] Dzyubenko A B, Mandray A, Huant S, Sivachenko A Yu and Etienne B 1994 *Phys. Rev.* B **50** 4687
[16] Szwacka T, Blinowski J and Betancur J 1995 *J. Phys.: Condens. Matter* **7** 4489
[17] Monozon B S 2001 *Superlatt. Microstruct.* **29** 17
[18] Ruan W Y, Chan K S and Pun E Y B 2001 *J. Phys.: Condens. Matter* **13** 1329
[19] Ruan W Y, Chan K S and Pun E Y B 2001 *Phys. Rev.* B **63** 205204
[20] Lin C D 1975 *Phys. Rev.* A **12** 493
[21] Lin C D 1976 *Phys. Rev.* A **14** 30
[22] Hornos J E, MacDowell S W and Caldwell C D 1986 *Phys. Rev.* A **33** 2212
[23] De Groote J J, Hornos J E, Coelho H T and Caldwell C D 1992 *Phys. Rev.* B **46** 2101
[24] Tang Jian-zhi, Watanabe S and Matsuzawa M 1992 *Phys. Rev.* A **46** 2437
[25] Lin C D 1995 *Phys. Rev.* **257** 2
[26] Masili M, Hornos J E and De Groote J J 1995 *Phys. Rev.* A **52** 3362
[27] De Groote J J, dos Santos A S, Masili M and Hornos J E 1998 *Phys. Rev.* B **58** 10 383
[28] De Groote J J, Masili M and Hornos J E 1998 *J. Phys. B: At. Mol. Opt. Phys.* **31** 4755
[29] Masili M, De Groote J J and Hornos J E 2000 *J. Phys. B: At. Mol. Opt. Phys.* **33** 2641
[30] De Groote J J, Masili M and Hornos J E 2000 *Phys. Rev.* A **62** 032508
[31] dos Santos A S, Masili M and De Groote J J 2001 *Phys. Rev.* B **64** 195210
[32] Starace A F and Webster G L 1979 *Phys. Rev.* A **19** 1629
[33] Coelho H T and Hornos J E 1991 *Phys. Rev.* A **43** 6379
[34] Macek J 1968 *J. Phys. B: At. Mol. Phys.* **1** 831
[35] Pekeris C L 1962 *Phys. Rev.* **126** 1470
[36] Wang L X, Kong X J, Li Y X and Xie S J 2001 *J. Phys.: Condens. Matter* **13** 8765